 doi:10.20944/preprints202111.0417.v2

Article

Martensitic phase transition in yttrium-stabilized ZrO_2 nanopowders by adsorption of water

E.B. Asgerov [1,2], A.I. Beskrovnyy [1], N.V. Doroshkevich [1,3], C. Mita [4], D.M. Mardare [4], D. Chicea [5], D. Lazar[6], A.A. Tatarinova [1], V.A. Alexandrov [1,7], S.I. Lyubchyk [8], S.B. Lyubchyk [8,9], A.I. Lyubchyk [9,10]*, A.S. Doroshkevich [1,11]

[1] Joint Institute for Nuclear Research, Dubna, Russia
[2] National Center for Nuclear Research, Baku, Azerbaijan
[3] Donetsk National Vasyl Stus University, Vinnitsa, Ukraine
[4] Alexandru Ioan Cuza University of Iasi, Faculty of Physics, Romania Bulevardul Carol I nr. 11, Iași 700506
[5] Research Center for Complex Physical Systems, Faculty of Sciences, "Lucian Blaga" University of Sibiu, Dr. Ion Ratiu str. no. 5–7, 550012, Sibiu, Romania
[6] National Institute for Research and Development of Isotopic and Molecular Technologies, Cluj-Napoca, România
[7] Dubna State University, Dubna, Russia, valdir-02@mail.ru
[8] REQUIMTE, Faculdade de Ciências e Tecnologia, Universidade Nova de Lisboa, Quina de Torre, 2829-516 Caparica, Portugal
[9] Research Centre in Industrial Engineering Management and Sustainability, Lusófona University, Campo Grande, 376 1749-024 Lisboa, Portugal
[10] Nanotechcenter LLC, Krzhizhanovsky str., 3, Kyiv 03680, Ukraine
[11] Donetsk Institute for Physics and Engineering named after O.O. Galkin, Kiev, Ukraine, doroh@jinr.ru
* Correspondence: p6193@ulusofona.pt

Abstract: The present study was aimed at revealing the influence of the mechanical stress induced by water molecules adsorption on the composition of crystalline phases in the ZrO_2–3mol%Y_2O_3-nanoparticles. Three basic methods have been used to determine the phase transition: neutron diffraction, Raman microspectroscopic scanning, and X-ray diffraction. The fact of phase-structural $\beta \rightarrow \alpha$ transformation and the simultaneous presence of two polymorphic structural modifications (β is the phase of the tetragonal syngony and α of monoclinic syngony in nanosized particles (9nm)) under normal physical conditions was established by these methods. Satisfactory consistency was achieved between the results obtained using different techniques.

Keywords: nanopowders; zirconium oxide nanoparticles; adsorption phase transition; polymorphism in zirconium dioxide; size effect of structural stabilization

1. Introduction

Due to the development of nanotechnology, the study of subtle structural effects associated with exposure of external physical factors to nanoscale objects became relevant [1, 2]. An extremely interesting object in this aspect is nanostructured systems based on zirconium oxide under hydration conditions. The adsorption of water on the nanoparticles surface leads to the destruction of ZrO_2-ceramics as a result of propagation of the $\beta \rightarrow \alpha$ (tetragonal-monoclinic, t-m) phase transformation from the surface to bulk of the material [2]. This transformation has a martensityc character, i.e. go forward at the speed of sound and requires a certain amount of material for the accumulation of required amount of elastic stresses [3, 4]. It is commonly assumed that in nanoparticles smaller than 30 nm t-m transformations cannot be realized due to the lack of the necessary volume for accumulation of stresses and propagation of the phase transformation front [5, 6]. However, the results of [7, 8], in which the effect of the so-called "chemoelectronic conversion" was shown, indicates that the t – m transformation still can be able in nanoscale objects. The confirmation of this fact is extremely interesting task as for fundamental science as for applications, in particular, adsorption electronics, alternative

 doi:10.20944/preprints202111.0417.v2

energetics and so on. In particular, changing parameters of the crystal lattice are accompanied by energy exchange of the nanopowder system with the external environment, which is extremely interesting for practical applications (electronics, power engineering).

The study of such adsorption transformation is a technically complex task. The general problem of the study of nanostructured systems by diffraction methods (X-ray, neutronography) is the large incoherent scattering ability of nanosized crystals (form-factor) and the high level of surface mechanical stresses due to presence of an adsorption hydrate shell which is covered the nanoparticles surface. As a result, diffraction patterns from nanostructured objects contain a large level of incoherent background and have a low intensity of reflexes. The intensity of the m-phase reflexes induced by water adsorption usually not exceeds error level, which does not allow identify unambiguously the considered adsorption effect by use of single method.

The methods themselves also have an individual limitation. The limitations of the applicability of XRD methods are connected to relatively small depth of X-ray penetration (limited to a surface layer of 20 nm).

Such a "surface" study often gives distorted information about the structure of bulk layers of a material, especially if there is a gradient of properties (a gradient in the size and chemical composition of ceramic grains, inhomogeneous hydration of compacts, etc.). Neutronography due to the relatively high penetrating power of neutrons (due to the relatively small scattering cross-section) at the same resolution (0,01%) allows to collect information from a significantly larger volume of material than in the case of XRD. However, use of neutron diffraction in these studies is limited by the absorption of neutrons by water molecules. This problem is partially solved by the replacement of water to deuterium. It should be noted that the obtaining of the diffraction pattern in X-ray diffractometry and neutronography is carried out in different ways (by a variation of the 2θ angle and using TOF method, respectively). Consequently, weak reflexes recorded by several methods in the region of the corresponding interplane distances are very likely to indicate they belonging to the desired phase. Thus, the combined use of X-ray diffraction and neutronography methods will significantly increase the probability of detecting small effects in nanopowder objects.

In addition, an alternative to diffraction methods is a spectrometric method for conducting structural studies. In particular, the method of Raman light scattering, which has proven itself in structural studies. Raman light scattering methods are sensitive to the short-range ordering of the arrangement of atoms in a structure and make it possible to investigate the subtle features of the real structure of crystals. The vibrations of complex anions in the crystal structure, the bonding forces inside of which considerably exceed the bonding forces with the cation sublattice are studies with their help. In this case, isomorphic substitutions in cationic positions affect to the position of vibration bands of complex anions. Knowing the spatial group of the crystal and the group of positional symmetry of a complex ion in the structure, it is possible to calculate the number of vibration bands of this ion in the main spectral regions. Those peculiarities of interaction with the substance of radiation (in the optical and X-ray ranges) and particles (neutrons), as well as various principles of obtaining and processing data allow to obtain a set of data required for unambiguous identification of the phase composition of nanoscale objects.

The aim of present work is establishing of a weakly expressed adsorption-induced phase transformation in a YSZ-nanopowder system using individual features of the listed sensitive analytical methods.

Preprints (www.preprints.org) | NOT PEER-REVIEWED | Posted: 1 December 2021 doi:10.20944/preprints202111.0417.v2

2. Materials and Methods

Interventionary studies involving animals or humans, and other studies that require ethical approval, must list the authority that provided approval and the corresponding ethical approval code.

As an object of investigation a two types of compact sets obtained from ZrO_2+3mol%Y_2O_3 nanopowders were used.

Powders for both types of samples were prepared by co-precipitation method. Zirconium oxychloride was used for preparing of the first type of samples and the zirconium oxynitrate was used for preparing a second type of samples. After drying in a microwave oven and subsequent calcinations at 400°C for 2 hours in a convection heating furnace the powders were sealed by uniaxial pressure (P = 40MPa) and after that by high hydrostatic pressure (HHP = 500MPa). So, investigated samples were compact sets in the form of tablets with diameter d = 16 mm and height h = 2 mm. Structure of powders and compact sets were investigated by X-ray diffraction (XRD) using a PANalytical device. Investigations of topology of samples were carried out by scanning (SEM) and transmission (TEM) electron microscopy using JSM640LV and JEM-200A (JEOL) devices respectively. Objects for TEM were prepared by two-stage replicas method. Moisture content in powder was determined by thermogravimetric analysis (TGA) using a specialized weights ADS50 (AXIS) at 120°C.

Used materials and research methods. To obtain nanopowders, chemical co-precipitation technology modified by physical actions was used [26]. At first, zirconium hydroxide was obtained by co-precipitation from chloride raw materials. After dehydration in a specialized microwave oven (T = 120 °C, t = 0,4 h), the amorphous powder underwent crystallization was annealed at 400 °C for 2 hours.

The spatial structural organization of the samples was studied by transmission electron microscopy (TEM) JEOL, JEM 200A).

The Raman LabRAM HR Evolution Horiba spectrometer at a wavelength of the emitting laser of 633 nm was used for determining of phase composition of Zirconium dioxide powders after drying and addition of deuterated water. The spectra were recorded at room temperature in the region of 150 – 1200 cm^{-1}. All measurements were performed in triplicate, the averaged spectra were used in the calculations. Processing was carried out using the computer program Origin 9.2.

The crystal structure of the nanostructured powder samples in X-ray frequency range was studied using an Empyrean PANalytical X-ray diffractometer with a CuKα radiation emitted using a Ni filter. Neutron diffraction experiments were carried out on the diffractometer DN-2, located on a high-flux pulsed neutron reactor IBR-2 (LNP named I.M. Frank, JINR, Dubna RF) [25]. The diffraction patterns were measured at a scattering angle of $2\theta = 174°$. The measurement time of one diffraction pattern was 12 hours. To record the diffraction patterns, the time-of-flight method was used; the total neutron flux on the sample was $5 \cdot 10^6$ n/sm^2·s, the spatial resolution $\Delta d/d$ at the interplanar distance at a scattering angle of $2\theta = 174°$ is close to 0,01. Neutron diffraction data were processed by the Rietveld method using the FullProf program.

Diffraction patterns were measured in humid conditions at room temperature, and in a dry state at 200 °C. For neutron and X-ray diffraction measurements, the samples were hydrated in a deuterium vapor atmosphere for 24 hours. The samples adsorbed up to 10–15 wt% of deuterium. The profile of the diffraction peaks of X-ray was adjusted in the range $30° < 2\theta < 45°$ using a Lorentzian peak functions without imposing any structural constraint.

Used calculating formalism. X-ray diffraction procedure. The ratio of the integrated peak intensities I^m_{111}, I^m_{-111}, I^t_{101} used to calculate the XRD-derived monoclinic volume fraction V^m. The molar fraction of the content of M-ZrO_2 was calculated as:

$$X^m = \frac{I^m_{111} + I^m_{-111}}{I^m_{111} + I^m_{-111} + I^t_{101}}$$

Preprints (www.preprints.org) | NOT PEER-REVIEWED | Posted: 1 December 2021 doi:10.20944/preprints202111.0417.v2

where I^m_{111}, I^m_{-111} are the intensity of the peaks representing the crystal orientation (111) and (–111) of M-ZrO_2, I^t_{101} is the intensity of T-ZrO_2 with the crystal orientation of (101) [27].

The volumetric fractions of the M-ZrO_2 and T-ZrO_2 phases from the intensities of the diffraction peaks (111) and (–111) of monoclinic and line diffraction (101) tetragonal was calculated as:

$$V^m = \frac{1{,}31X^m}{1+0{,}31X^m}$$

For a proper application of this equation, a fitting procedure of the X-ray pattern makes using a Lorentzian or Gaussian curve in order to determine peaks intensity. In the ZrO_2 tetragonal $P4_2/nmc$ structure, the six atoms localized in the following special positions – 4d for oxygen corresponds to a tetrahedral site centered on Zr(Y) atoms and 2a for Zirconium.

Neutron diffraction. The energy spectrum of slow neutrons has a continuous (Maxwell) character [28]. The time of flight (TOF-method) was used to the analysis of the slow neutron energy as a slow neutron source a pulsed nuclear reactor IBR-2 was used. The position of the diffraction peaks on the time scale was determined by the condition:

$$t = \frac{L}{v} = \frac{\lambda mL}{h} = \frac{2mld_{hkl}\sin\theta}{h}$$

where L is the total transit distance from the neutron source to the detector, v is the neutron velocity, λ is the neutron wavelength, m is the neutron mass, h is the Planck constant, d_{hkl} is the interplanar distance, θ is the Bragg angle.

Functional dependence of the resolution R on the interplanar distance d (or the transmitted pulse Q) [29] was calculated as:

$$R = \frac{\Delta d}{d} = \sqrt{\left(\frac{\Delta t_0}{t}\right)^2 + \left(\frac{\Delta\theta}{tg\theta}\right)^2 + \left(\frac{\Delta L}{L}\right)^2}$$

where Δt0 is the neutron pulse width, t = 252,778 Lλ – is the total time of flight (μs), L is the flying distance from the source to the detector (m), λ is the neutron wavelength (Å), θ is the Bragg angle.

Raman Spectroscopy. The following model representation of the ZrO_2-Raman spectrum was used:

$$\Gamma = A_{1g} + 2B_{1g} + 3E_{1g}$$

where: A_{1g} – a mode of the oxygen motions along the z-direction only; B_{1g} – a modes are includes Zirconium and Oxygen displacement in the z-direction; E_{1g} – a modes are consists in displacements of Oxygen and Zirconium in the (x, y) plane [30]. According to the Group theory there are 36 lattice vibrational modes for monoclinic ZrO_2 including infrared, acoustic and others [31]:

$$\Gamma = 9A_g + 9A_u + 9B_g + 9B_u$$

Monoclinic doublet at 181 cm^{-1} and 190 cm^{-1} and with the adjacent tetragonal peak at 147 cm^{-1} commonly used for the quantitative determination of monoclinic phase:

$$V^m = \sqrt{0{,}19 - \frac{0{,}13}{X^m - 1{,}01} - 0{,}56} \quad \text{with} \quad X^m = \frac{I^m_{181} + I^m_{190}}{I^m_{181} + I^m_{190} + I^t_{147}}$$

where I^m_{181}, I^m_{190}, and I^t_{147} are represent the integrated intensity of the monoclinic 181 cm^{-1} and 190 cm^{-1} and tetragonal 147 cm^{-1} peaks, respectively. A common procedure was consisted in plotting the monoclinic volume fraction V^m of the wet specimens against the monoclinic/tetragonal intensity ratio Xm measured from the Raman spectra [32].

3. Results

 doi:10.20944/preprints202111.0417.v2

This section may be divided by subheadings. It should provide a concise and precise description of the experimental results, their interpretation, as well as the experimental conclusions that can be drawn.

There are many opinions regarding the mechanism of T-phase stabilization in the YSZ system. In [9-11] an explanation and experimental proof of the stabilization of ZrO_2 in the cubic phase due to the nonstoichiometry of oxygen vacancies is given. The essence of such stabilization by nonstoichiometric defects is that, if the required concentration of anion vacancies is created in the material, then the local stresses arising in this case can keep the high-temperature cubic phase at room temperature. Obviously, this explanation is also applicable to the stabilization of β-ZrO_2 [12]. In this case, nonstoichiometry is the main factor determining the stability of high-temperature phases. A number of researchers believe that the existence of high-temperature ZrO_2 phases under normal conditions can be due to the stabilizing effect of impurities. Thus, in [13] reported enhancement of the formation and existence of high-temperature phases for the corresponding oxides through the interaction of Zr^{4+}, Hf^{4+}, Th^{4+}, U^{4+} ions with water and hydroxyl ions. This point of view is also expressed in [14, 15]. A similar stabilizing effect is exerted by metal oxides dissolved in ZrO_2, the presence of which in the lattice also leads to the appearance of oxygen vacancies [16]. It is believed that in this case a stabilizing effect is exerted by the stresses created by oxygen vacancies, as in the case of nonstoichiometric stabilization.

An explanation of the stabilization of high-temperature phases of ZrO_2 can be given within the framework of the energy theory [17-19] from the standpoint of thermodynamics. Since the internal crystal energy U consists of the energy of the inner part of the crystal U_v and the surface energy σS (σ is the specific surface energy; S is the surface area), $U = U_v + \sigma S$ and $U_{v\alpha} < U_{v\beta} < U_{v\gamma}$, and $\sigma_\alpha > \sigma_\beta > \sigma_\gamma$, then for $S < S_{cr}$ at room temperature, the high-temperature phase can be energetically favorable, i.e., the smaller the particle size of the high-temperature phase, the more stable it is. This approach makes it possible to explain the reversibility of the T-M transformation process in nanoparticles. Obviously, the reverse process (T-M transformation) cannot be realized in massive bodies precisely because of the negligible surface energy. The thermodynamic approach allows us to draw another important conclusion about the mechanism of T-M transformation in nanoparticles: for it to be realized, it is necessary to change the surface energy of the nanoparticle significantly. The probable mechanisms of this process are associated with a change in the physicochemical and electronic properties of the surface of nanoparticles by adsorbates (OH-groups) (Adsorption mechanism of T-M phase transformation [7–8, 12]). Estimates of the corresponding structural parameters (level of microstresses, sizes of unit cells, etc.) will provide quantitative information about the forms of manifestation of the mechanism of T-M transformation from the standpoint of crystallography.

Electron microscopy data. A typical electron microscopic image of the studied powders is shown in Fig. 1. It can be seen that particles of the order of 9 nm are uniform in size and relatively well separated.

Neutron diffraction data. Neutron diffraction patterns of dry and hydrated ZrO_2+3mol%Y_2O_3 are shown in Fig. 2. The analysis of neutron data showed that the nanostructured system saturated of deuterated water under normal physical conditions is in the tetragonal crystalline symmetry system $P4_2/nmc$. It should be noted the presence of a small amount of the monoclinic phase with P2/c symmetry. The values of the parameters of the unit cell of the tetragonal and monoclinic phases calculated from the diffraction data are given in Table 1. It can be seen that the desorption of deuterium leads to the disappearance of the reflexes d_{hkl} = 1.47 Å, d_{hkl} = 1.97 Å и d_{hkl} = 2.27 Å, d_{hkl} = 2.67 Å, d_{hkl} = 3.17 Å corresponding to the M-phase on the diffraction patterns. Thus, a model experiment with heating shows that annealing at 200°C leads to complete reduction of the m- phase (~8% M-phase) from YSZ-nanopowders. This effect confirms the above considerations regarding the destabilization of the T-phase by adsorbates. Vertical lines indicate the calculated positions of the structural diffraction peaks. The most intense peaks are denoted by the symbols «M» and «T» (respectively, of the monoclinic and

 doi:10.20944/preprints202111.0417.v2

tetragonal phases). Parameters of elementary cells of M- and T-phases in the ZrO_2–3mol%Y_2O_3 nanopowders, obtained from neutron spectra are given in Table 1.

X-ray data. The XRD diffraction patterns of YSZ – nanopowders obtained under different conditions are shown in Fig. 3. The structure of dry sample was identified as tetragonal. The presence of the M-phase in samples saturated with water moisture is very weak. To determine the quantity of the M-phase, the mathematical apparatus given in "Materials and Methods" section was used. The value of m phase was found as V_m ~ 3 – 4% according to equation (4) which indicates that the adsorption-induced phase transformation affects only a small part of the volume of material Parameters of elementary cells of M- and T-phases in the ZrO_2–3mol%Y_2O_3 nanopowder with different degrees of moisture, obtained from X-ray spectra are given in Table 2.

Raman data. Dried at 200 °C nanopowder of ZrO_2+3mol%Y_2O_3 according to Raman spectroscopy data is represented by a T-ZrO_2 structural modification, which is well expressed by intense peaks at 150, 265, 322, 469 and 639 cm^{-1} (Fig. 4) [20, 21].

Peaks of the monoclinic phase were absent in this sample. The ratio of the tetragonal peaks I265/I316 intensity, which characterizes the ordering of the crystal lattice was 1.3 in this case. The ratio of the I262/I637 peaks intensity which characterizes a degree of tetragonality for this sample was 1.1. This fact confirmed the presence of the tetragonal phase only.

The Raman spectrum of deuterated nanpowder corresponded to a mixture of tetragonal and monoclinic phases. Detected well-pronounced intense peaks at 148, 262, 316, 471, and 637 cm^{-1} are corresponded of the T-ZrO_2 phase. A slightly shifting (2 cm^{-1}) to the low-frequency region compared with the peaks of dry powder indicated the presence of distortions in the crystal lattice, especially in Zr–O (Y–O) bonds. The low-intensity peaks at 219, 542, 562 cm^{-1}, and a series of weakly intense peaks of H-group (708, 783, 835, 859, 872, 955, 1145, 1167 cm^{-1}), C-group (100 – 700 cm^{-1} region) and S-mode (1040 – 1050 cm^{-1} region) are corresponded of the M-ZrO_2 phases [22, 23, 24]. The ratio of the intensities of the peaks of the tetragonal I262/I316 modification in this sample is 1.4, and the ratio of the intensities of the peaks I262/I637 was 0,9, which confirms the presence of two phases. The estimated (equation 6) quantity of M-ZrO_2 phase is about ~ 5%.

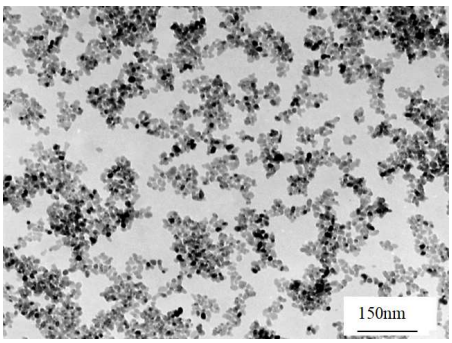

Figure 1. TEM images of a nanopowder of the composition ZrO_2–3mol%Y_2O_3, 400°C. 2h.

Preprints (www.preprints.org) | NOT PEER-REVIEWED | Posted: 1 December 2021 doi:10.20944/preprints202111.0417.v2

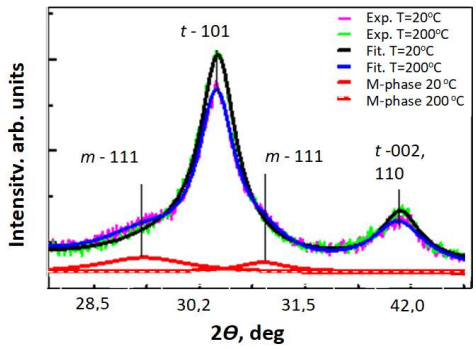

Figure 2. Neutron diffraction patterns of dry (black line, 2) and hydrated (blue line, 1) ZrO_2–3mol%Y_2O_3 nanopowder.

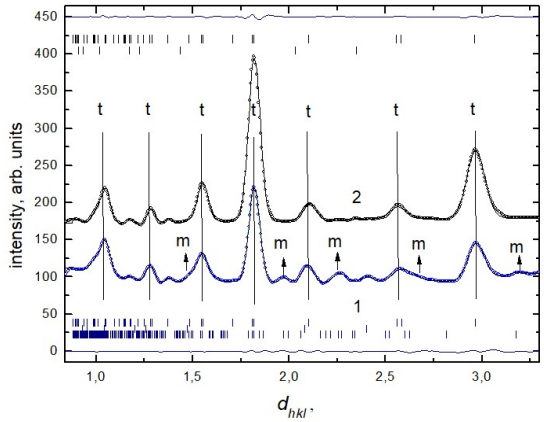

Figure 3. Experimental (green and purple lines), calculated (green and black lines) XRD diffraction patterns and mathematically selected M-phase signal (red lines) of ZrO_2–3mol%Y_2O_3 nanopowder sample, accordingly, after saturating and drying at 200°C, 30 min.

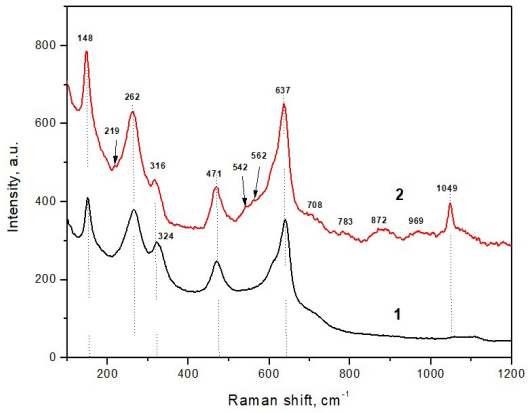

Figure 4. Raman spectra of dry (black line, 1) and deuterated (red line, 2) ZrO_2–3 mol%Y_2O_3 nanopowders.

Preprints (www.preprints.org) | NOT PEER-REVIEWED | Posted: 1 December 2021 doi:10.20944/preprints202111.0417.v2

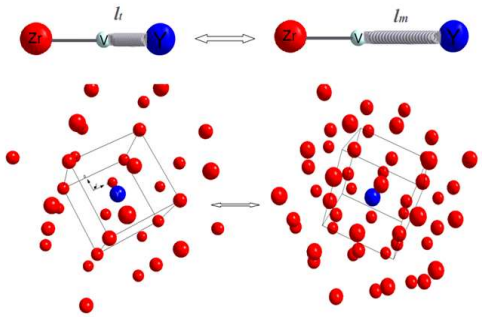

Figure 5. Schematic representation of the T-M transformation in ZrO_2: lt and lm are the yttrium (Y) - oxygen vacancy (V) bonds length in T- and M-structural modifications.

Table 1. Parameters of elementary cells of T- and M-phases in the ZrO_2–3 mol%Y_2O_3 nanopowder according to neutron diffraction data.

	a	b	c	α	β	γ
T-phase	3.621	3.621	5.178	90.00	90.00	90.00
M-phase	5.128	5.246	5.288	90.00	100.16	90.00

Table 2. Parameters of elementary cells of T- and M-phases in the ZrO_2–3 mol%Y_2O_3 nanopowder with different degrees of moisture.

	a	b	c	α	β	γ	Volume
T-phase (dry)	3.612	3.612	5.186	90.00	90.00	90.00	67.659
T-phase (wet)	3.610	3.610	5.182	90.00	90.00	90.00	67.532
M-phase (wet)	5.118	5.241	5.274	90.00	100.18	90.00	141.467

4. Discussion

Thus, Raman spectroscopy confirmed neutron and X-ray diffractions data about adsorption-induced formation of the monoclinic phase in ZrO_2–3mol%Y_2O_3 nanopowders. A probable mechanism of tetragonal-monoclinic phase transformation in ZrO_2-nanoparticles was discussed in [7-8] and is showed schematically on Fig. 5. In opinion of authors, during adsorption processes, water molecules through the donor-acceptor interaction with impurity cations Y^+ leads to the localization of electrons from the local energy levels of surface atoms, thereby destroying the T-phase stabilizes bond between impurity ions $Y^{3+(-)}$ and oxygen vacancies $V^{-(+)}$ [4] (Fig. 5). As can be seen from Table 2 the adsorption of water leads to a decrease in the volume of the crystal lattice cells of the t-phase by an amount of the of 0,127A or 0.19%. Thus, it can be concluded that the adsorption of moisture leads to the densification of the surface layer of the material of nanoparticles with respect to the volume, presumably as a result of the collapse of vacancies after localization of some electrons from the lattice to the energy levels of adsorbate. The subsequent increase in the internal energy of the crystal obviously leads to the destabilization of the metastable T-phase and the formation of an equilibrium m-phase in an amount proportional to the probability of localization of electrons at the adsorption levels of adsorbates. described by the Fermi - Dirac statistics [2].

The established effect as one of the forms of recharging of oxide nanoparticles surface layer, confirms the adsorption mechanism of electron emission in ZrO_2–3mol%Y_2O_3 described in [7, 8, 33, 34].

The question of the established t - m transformation mechanism realization remains open. For a better understanding of this phenomenon, additional analysis of the process mechanism and its thermodynamic are necessary. Obtained results provide new perspectives in the fundamental and applied aspects of powder nanotechnologies.

5. Conclusions

 doi:10.20944/preprints202111.0417.v2

Using the methods of Raman spectroscopy, neutron and X-ray diffraction methods a unique T-M phase transformation in nanosized YSZ objects upon water adsorption was established. The M-ZrO_2 phase appearing at a quantity of is about ~ 5% after moisture saturation from gas-atmosphere under normal physical conditions was shown.

The decrease of the volume of the crystal lattice cells of the T-phase at an amount of 0.19% as a result of moisture adsorption by surfaces was established.

The assumption about the connection of the physical mechanism of transformation of the extremely nonequilibrium surface of nanoparticles with the collapse of vacancies in the near-surface layer due to the donor-acceptor interaction of the electron subsystem of nanoparticles with the adsorption layer ($Y^{3+(-)}$ – $V^{-(+)}$ - bond) was made.

The possibility of adsorption of hydroelectric conversion by transformational mechanism was shown by the example of ZrO_2–3mol%Y_2O_3 nanocrystals.

6. Patents

Author Contributions:

Asgerov E.B. - Analysis and mathematical processing of the results, preparation of the manuscript, discussion of the empirical mechanism of the effect of adsorption-induced phase transformation.

Doroshkevich A.S. - Development of the empirical mechanism of the effect of adsorption-induced phase transformation, discussion of the results of the experiment.

Beskrovnyy A.I. - Neutron experiment, discussion of experimental results.

Mardare D.M. - Comprehensive analysis of the results, discussion of the mechanisms T-M transformation in YSZ from the standpoint of crystallography.

Lyubchyk A.I. - TEM - research samples, discussion of the experimental results from the standpoint of low-dimensional systems physic.

Lazar D. - XRD - research of samples, discussion of the results of the experiment.

Lyubchyk S.I. - Comprehensive analysis of the results, analysis of the mechanism of the T-M transformation in YSZ from the standpoint of physical chemistry.

Mita C. – Analysis of a Raman spectra, discuss the results of the experiments from the standpoint of the crystal lattice symmetry theory.

Chicea D. - Comprehensive analysis of the results, discussion of the mechanism of T-M transformation from the standpoint of thermodynamics.

Doroshkevich N.V. - Obtaining a Raman scattering data, discuss the results of the experiments.

Alexandrov V.A. - Conduct a literature review, discuss the results of the experiment.

Tatarinova A.A. - Conduct a literature review, discuss the results of the experiment.

Lyubchyk S.B. – Conceptualization, Formal analysis, discuss the results of the experiment.

Acknowledgments: This work was supported by the Associate Laboratory for Green Chemistry - LAQV which is financed by national funds from FCT/MCTES (UIDB/50006/2020 and UIDP/50006/2020), H2020/MSCA/RISE/SSHARE number 871284 project and the RO-JINR Grant No. 367 / 2021 item 27 and RO-JINR Projects № 366 / 2021 items 57, 61, 83, 85

Conflicts of Interest: The authors declare no conflicts of interests.

References

1. Gusev, A. I. *Nanomaterials, Nanostructures, and Nanotechnologies*; Fizmatlit: Moscow, Russia, **2007**
2. Alekseenko, V. I., Volkova, G. K. Adsorption mechanism of phase transformation of stabilized zirconium dioxide. *Technical Physics* **2000**, *70*, 57–62
3. Konstantinova, T. E., Volkova, G. K., Danilenko, I. A. Features of the tetragonally monoclinic transformation in the surface layers of the ceramics of the ZrO_2-Y_2O_3 system. *PHPT* **1996**, *17*, 9–19
4. Chevalier, J., Gremillard, L., Virkar, A. V., Clarke, D. R. The tetragonal-monoclinic transformation in zirconia: lessons learned and future trends. *J. Amer. Ceram. Soc.* **2009**, *92*, 1901–1920

5. Petrunin, V. F. et al. Neutron structural study of ultradispersed zirconium dioxide powders. *Powder Metallurgy* **1989**, *3*, 46-50
6. Shevchenko, V. Ya., Malochkin, O. V., Panov, V. S., Barinov, S. M. Size effect in sol-gel synthesis of ultrafine zirconia stabilized by ytterbium oxide. *Reports of Academy of Sciences* **1999**, *365*, 649–652
7. Lyubchyk, A. et al. Experimental evidence for chemo-electronic conversion of water adsorption on the surface of the nanosized yttria stabilized zirconia. Phys. Chem. Appl. Nanostruct. **2017**, 257–262
8. Doroshkevich, A. S. et al. Chemical-electric energy conversion effect in zirconia nanopowder systems. *J. Synch. Investig.* **2017**, *11*, 523–529
9. Vishnevsky I.I., Gavrish A.M., Sukharevsky B.Ya., On a possible mechanism for stabilizing the cubic ZrO2 *Tr. Ukr. Research Institute of Refractories* **1962**, *6*, *53*, 74–80
10. Livage J., Mazieres Ch., *C.r. Acad. Sci.* **1965**, *261*, *21*, 4433–4435
11. Denoux M., *C.r. Acad. Sci.* **1965**, *260*, *19*, 5003–5005
12. V.I. Alekseenko, G.K. Volkova, Adsorption Mechanism of Phase Transformation of Stabilized Zirconium Dioxide, *Technical Physics* **2000**, *70*, *9*, 57–62
13. Mumpton F., Roy R., *J. Amer. Ceram. Soc.* **1960**, *43*, *5*, 234–240
14. Glushkova V.B., *Rare earth metals, alloys and compounds*; Science: Moscow, Russia, 1973; pp. 216–217
15. Ch. L. Gremillardw. The Tetragonal-Monoclinic Transformation in Zirconia: Lessons Learned and Future Trends Jerome, *J. Am. Ceram. Soc.* **2009**, *92*, *9*, 1901–1920
16. Hund F., X-ray conductivity and density of fluorite phase of system ZrO_2-Y_2O_3 *J. Electrochem. Soc.* **1951**, *55*, 363–367
17. Krauth A., Meyer H., *Ber. Dt. Reram. Ges. Bd.* **1965**, *42*, *3*, 61–72
18. Strekalovsky V.N., Polezhaev Yu.M., Palguyev S.F. *Oxides with impurity disordered. Composition, structure, phase transformations*, Science: Moscow, Russia, **1967**
19. Shukla S., Seal S. Mechanisms of room temperature metastable tetragonal phase stabilisation in zirconia. *International Materials Reviews* **2005**, *50*, *1*
20. Siu G. G., Stokes M. J., Liu Y. L. Variation of fundamental and higher-order Raman spectra of ZrO2 nanograins with annealing temperature. *Phys. Rev.* **1999**, *59*, 3173
21. Li, M., Feng, Z., Xiong, G., Ying, P., Xin, Q., Li, C. Phase transformation in the surface region of zirconia detected by UV Raman spectroscopy, *J. Phys. Chem.* **2001**, *105*, 8107–8111
22. Kumari, L., Li, W., Wang, D. Monoclinic zirconium oxide nanostructures synthesized by a hydrothermal route. *Nanotechnology* **2008**, *19*, 195602
23. Paul, A., Vaidhyanathan, B., Binner, J. Micro - Raman spectroscopy of indentation induced phase transformation in nanozirconia ceramics. *Adv. Appl. Ceram.* **2011**, *110*, 114–119
24. Zhang P., Choy K.-L. The synthesis of single tetragonal phase zirconia by sol-gel route. *IJOER* **2015**, *1*, 18–24
25. Balagurov A.M. et al. Neutron diffractometer for real-time studies of transient processes at the IBR-2 pulsed reactor. *J. Synch. Investig.* **2016**, *10*, 467–479
26. Konstantinova, T. et al. Mesoscopic phenomena in oxide nanoparticles systems: processes of growth. *J. Nanopart. Res.* **2011**, *13*, 4015–4023
27. Toraya, H., Yoshimura, M., Somiya, S. Calibration Curve for Quantitative-Analysis of the Monoclinic-Tetragonal ZrO_2 System by X-Ray-Diffraction. *J. Amer. Ceram. Soc.* **1984**, *67*, 119–121
28. Bokuchava, G. D., Petrov, P. & Papushkin, I. V. Application of neutron stress diffractometry for studies of residual stresses and microstrains in reactor pressure vessel surveillance specimens reconstituted by beam welding methods. *J. Synch. Investig.* **2016**, *10*, 1143–1153
29. Balagurov, A. M., Bobrikov, I. A., Bokuchava, G.D., Zhuravlev, V. V., Simkin, V. G. Correlation Fourier diffractometry: 20 Years of experience at the IBR-2 reactor. *Phys. Part. Nuclei.* **2015**, *46*, 249–276
30. Negita, K., Takao, H. Condensations of phonons at the tetragonal to monoclinic phase transition in ZrO_2. *J. Phys. Chem. Solids.* **1989**, *50*, 325–331
31. Anastassakis, E., Papanicolaou, B., Asher, I. M. Lattice dynamics and light scattering in Hafnia and Zirconia. *J. Phys. Chem. Solids.* **1975**, *36*, 667-676
32. Kim, B. K., Hahn, J. W. & Han, K. R. Quantitative phase analysis in tetragonal-rich tetragonal/monoclinic two phase zirconia by Raman spectroscopy. *J. Mater. Sci. Lett.* **1997**, *16*, 669–671
33. Subhoni, M. et al. Density functional theory calculations of the water interactions with ZrO_2 nanoparticles Y_2O_3 doped. *J. Phys.: Conf. Ser.* **2018**, *994*, 12–13
34. Doroshkevich, A. S. et al. Nonequilibrium chemo-electronic conversion of water on the nanosized YSZ: experiment and molecular dynamics modelling problem formulation. *J. Phys.: Conf. Ser.* **2017**, *848*, 12–21